

Californian forest fire plumes over Southwestern British Columbia: lidar, sunphotometry, and mountaintop chemistry observations

I. McKendry¹, K. Strawbridge², M. L. Karumudi³, N. O'Neill³, A. M. Macdonald⁴, R. Leaitch⁴, D. Jaffe⁵, P. Cottle¹, S. Sharma⁴, P. Sheridan⁶, and J. Ogren⁶

¹Department of Geography, the University of British Columbia, Vancouver, British Columbia, Canada

²Science and Technology Branch, Environment Canada, Centre for Atmospheric Research Experiments, Egbert, Ontario, Canada

³Université de Sherbrooke, Sherbrooke, QC, Canada

⁴Science and Technology Branch, Environment Canada, 4905 Dufferin Street, Toronto, Ontario M3H 5T4, Canada

⁵Atmospheric and Environmental Chemistry, University of Washington-Bothell, Seattle, USA

⁶NOAA-Earth System Research Laboratory, Global Monitoring Division, Boulder, Colorado, USA

Received: 8 July 2010 – Published in Atmos. Chem. Phys. Discuss.: 2 September 2010

Revised: 16 December 2010 – Accepted: 19 December 2010 – Published: 17 January 2011

Abstract. Forest fires in Northern California and Oregon were responsible for two significant regional scale aerosol transport events observed in southern British Columbia during summer 2008. A combination of ground based (CORALNet) and satellite (CALIPSO) lidar, sunphotometry and high altitude chemistry observations permitted unprecedented characterization of forest fire plume height and mixing as well as description of optical properties and physico-chemistry of the aerosol. In southwestern BC, lidar observations show the smoke to be mixed through a layer extending to 5–6 km a.g.l. where the aerosol was confined by an elevated inversion in both cases. Depolarization ratios for a trans-Pacific dust event (providing a basis for comparison) and the two smoke events were consistent with observations of dust and smoke events elsewhere and permit discrimination of aerosol events in the region. Based on sunphotometry, the Aerosol Optical Thicknesses (AOT) reached maxima of ~ 0.7 and ~ 0.4 for the two events respectively. Dubovik-retrieval values of $r_{\text{eff},f}$ during both the June/July and August events varied between about 0.13 and 0.15 μm and confirm the dominance of accumulation mode size particles in the forest fire plumes. Both Whistler Peak and Mount Bachelor Observatory data show that smoke events are accompanied by elevated CO and O₃ concentrations as well as elevated K⁺/SO₄ ratios. In addition to documenting the meteorology and physic-chemical characteristics of two regional scale

biomass burning plumes, this study demonstrates the positive analytical synergies arising from the suite of measurements now in place in the Pacific Northwest, and complemented by satellite borne instruments.

1 Introduction

Biomass burning plays an important role in the climate system and is the second largest source of anthropogenic aerosols (IPCC, 2001). Aerosols produced from the burning of forests, grasslands and crops scatter and absorb solar radiation (direct effect) while also influencing cloud processes by acting as cloud condensation nuclei (indirect effect). In addition, aerosols from biomass burning are a source of air pollution (including greenhouse gases) and may seriously degrade visibility regionally (e.g. Pahlow et al., 2005).

Physical, chemical and optical properties of biomass burning plumes have been studied extensively in a variety of global settings. This work is reviewed by Reid et al. (2005 a, b). In summary, approximately 80–90% of smoke aerosol volume is typically in the accumulation mode (particle diameter $< 1 \mu\text{m}$) with smoke particles primarily composed of organic carbon (50–60%) and black carbon (5–10%). However, the properties of smoke vary between fires, and are dependent on such variables as fuel type and moisture, combustion phase, and wind conditions. Furthermore, the physical, chemical, and optical properties of biomass-burning aerosols can change rapidly as they disperse. Typically, aged smoke particles are larger (volume mean diameters ranging



Correspondence to: I. McKendry
(ian@geog.ubc.ca)

from 0.26 to 35 μm) and more spherical than their fresh counterparts (Reid et al., 2005b).

Proliferation of both ground-based and satellite-borne remote sensing technologies such as lidar (light detection and ranging), and sunphotometry (AERONET, Aerosol Robotic Network) has led to significant advances in the understanding of biomass burning plumes, including their transport and dispersion over local to global scales, as well as their physical chemical and optical characteristics (see for example Amaridis et al., 2008; O'Neill et al., 2008). A milestone in the satellite remote sensing of aerosols occurred in April 2006 when the Cloud-Aerosol Lidar and Infrared Pathfinder Satellite Observation (CALIPSO) was launched into the A-train of instruments that also includes MODIS (or Moderate Resolution Imaging Spectroradiometer). Together these instruments provide an unprecedented capability to monitor global aerosols (including clouds).

In the North American context, the combination of novel satellite products, and ground-based lidar have been exploited to investigate forest fire plumes. For example, Hoff et al. (2007) have examined the transport of forest fire plumes from Alberta and the Yukon to Maryland using ground-based lidar, CALIPSO and MODIS data, whilst Duck et al. (2007) have examined the transport of fire emissions from Alaska and the Yukon territory to Nova Scotia. Similarly, Pahlow et al. (2008) examined the transport and boundary layer impacts of Quebec forest fires on the Baltimore region using ground-based lidar and MODIS. The impact of Pacific Northwest wildfires on air quality throughout North America has also been examined using CALIPSO, MODIS and the Regional Air quality Modelling System (RAQMS) by Kittaka et al. (2007).

In the Pacific Northwest, recent research (e.g. Jaffe et al., 2003) has focused on the trans-Pacific transport of pollutants (including aerosols of both anthropogenic and natural origin, the latter being primarily crustal dust emanating from the deserts of Asia, and occasionally North Africa). In southwestern British Columbia, whilst numerous studies have addressed spring trans-Pacific transport events (Hacker et al., 2001; McKendry et al., 2001, 2007, 2008; Holzer et al., 2003) little research has addressed the impact of regional biomass burning on local air quality. With establishment of the Whistler high altitude chemistry site in 2002 and the Vancouver CORAL-Net (Canadian Operational Research Aerosol Lidar network; www.coralnet.ca) lidar facility in 2008, complementing the AERONET/AEROCAN site on Saturna Island, opportunity exists for a more comprehensive examination of regional biomass burning events (AEROCAN is the Canadian sub-network of AERONET).

Given the coincidence of novel observing technologies (CALIPSO, CORAL-Net) and an active 2008 wild fire season in western North America (especially Northern California and Oregon), we specifically seek to:

- Document two cases of regional scale transport of biomass burning plumes from Northern California to Southwestern British Columbia and distinguish these from trans-Pacific dust events. A trans-Pacific dust event during 2008 provides a useful basis for comparison.
- Describe regional fire haze characteristics including vertical extent, impact on boundary layer aerosol concentrations and visibility, as well as physico-chemical and optical characteristics.
- Take the opportunity to compare and contrast CALIPSO depolarization data with higher resolution ground-based Lidar depolarization data.

2 Methods

2.1 Ground-based lidar (CORALNet)

CORALNet-UBC is a semi-autonomous lidar located at the western edge of the city of Vancouver on the grounds of the University of British Columbia (UBC) in close proximity to Georgia Strait (Fig. 1). The remotely controlled permanent facility is housed in a cargo trailer with modifications including a roof hatch assembly, basic meteorological tower, radar interlock system, climate control system and leveling stabilizers. The unit can be operated via an internet link and requires an external power source. A precipitation sensor is used to operate the roof hatch and three pan/tilt webcams capture sky conditions and monitor the lidar system's health. A remote control interface is used to control all vital components of the system, including the ability to provide hard resets of the laser electronics.

A Continuum Inlite III (small footprint) laser operating at 1064/532 nm simultaneously with a pulse repetition rate of 10 Hz is the foundation of the system. The energy output is approximately 150 mJ and 130 mJ at the emitting wavelengths of 532 nm and 1064 nm respectively. Backscatter information is collected at 3 m vertical resolution with 10 s averaging over a range from near ground to 15 km.

2.2 Cloud-Aerosol Lidar and Infrared Pathfinder Satellite Observation (CALIPSO)

The Cloud-Aerosol Lidar and Infrared Pathfinder Satellite Observation (CALIPSO) satellite provides new insight into the role that clouds and atmospheric aerosols (airborne particles) play in regulating Earth's weather, climate, and air quality. CALIPSO combines an active lidar instrument with passive infrared and visible imagers to probe the vertical structure and properties of thin clouds and aerosols over the globe (Vaughan et al., 2009). CALIPSO was launched on 28 April 2006 with the cloud profiling radar system on the CloudSat satellite. Version 3.01 data is used in the present study.

2.3 Lidar depolarization

Both CORALNet-UBC and CALIPSO provide depolarization information that may be used to discriminate aerosol shape characteristics. Transmitted lidar emits nearly 100% polarized light. However, the return signal may be significantly depolarized depending on the shape of the aerosols responsible for backscattering. Consequently the volume depolarization ratio provides a very useful means by which to discriminate between ice and water clouds and between aerosols having irregular shapes and those that are spherical. This property is a useful component of aerosol detection algorithms such as used in CALIPSO (Vaughn et al., 2008) and, in the context of this study, provides a basis for discriminating between smoke and dust plumes in lidar imagery. Previous studies suggest that depolarization from ice crystals is of the order of 30–50%, whereas for spherical water droplets depolarization is $\sim 0\%$ (i.e. original polarization of the lidar beam is preserved; Sassen, 2000). Smoke plumes from biomass burning typically have values of 0–10% (Murayama et al., 2003) but may be as high as 10–20% (Hoff et al., 2007; Sassen, 2000). Typically, the irregular shape of crustal dust aerosol produces significantly higher depolarization ratios ($>20\%$, Murayama et al., 2003).

2.4 Mountain-top chemistry observations

Measurements of particles and trace gases are made by Environment Canada at a high elevation site in Whistler, BC, approximately 100 km north of Vancouver (Fig. 1). The site is located at the top of a ski hill, at Whistler peak, 2182 m a.s.l. There are no continuous combustion sources at the peak and influences from snow vehicles have been identified and removed from the data set.

In 2008 the ongoing measurements at Whistler Peak were O_3 , CO, particle chemistry, particle size distributions (0.01–20 μm), light scattering and light absorption. Particle chemistry consisted of 48 h averaged filters cut at 2.5 μm and analyzed by ion chromatography (IC) for ions of chloride, nitrate, sulfate, sodium, ammonium, potassium, magnesium and calcium. Particle number and size distributions are measured using a TSI 3025 Condensation Particle Counter and a MSP Wide Range Spectrometer. Particle size distributions from 0.01 μm to 20 μm are measured using a Wide Range Particle Spectrometer (WPS; Model MSP-1000X; MSP Corporation). The MSP is verified using nearly monodisperse particles generated using a TSI 3071 Electrostatic Classifier. Ambient particles are sampled through a stainless steel manifold. The manifold intake is heated to a minimum of 4 $^{\circ}\text{C}$ in order to prevent rime of the intake when supercooled cloud is present. In addition, the aerosol is heated by being drawn into the room with the instruments; the temperature of the aerosol inside the room at the point of measurement is 20 $^{\circ}\text{C}$ to 25 $^{\circ}\text{C}$ compared with outside air temperatures between -10°C and 15 $^{\circ}\text{C}$ during the study. Particle volume scatter-

ing and backscatter coefficients $<2.5 \mu\text{m}$ are measured using a TSI 3563 Integrating Nephelometer. The instrument is calibrated approximately once a month. Particle light absorption is measured using a Particle Soot Absorption Photometer (PSAP) corrected for multiple scattering using the algorithm of Bond et al. (1999). These optical data are acquired and processed using NOAA ESTL software (NOAA website).

Mount Bachelor Observatory (MBO) is located on the summit of a dormant volcano in central Oregon (43.98 $^{\circ}$ N 121.7 $^{\circ}$ W, 2763 m.a.s.l.) (Fig. 1). Since establishment, MBO has proven to be well-positioned to observe Asian air pollution and biomass burning plumes (Weiss-Penzias et al., 2007). The sampling inlet is located on the roof of the summit lift building, and the instruments are located in a temperature controlled room within the building, situated approximately 15 m lower than the inlet. Multi-wavelength measurements of sub-micron dry aerosol scattering (σ_{sp}) and aerosol absorption (σ_{ap}) are measured using a three wavelength integrating nephelometer (Model TSI-3563, TSI Incorporated, Shoreview, MN) and a three wavelength Particle Soot Absorption Photometer (PSAP, Radiance Research, Seattle, WA).

2.5 Ancillary data

Back-trajectories from Vancouver were calculated using the HYSPLIT (HYbrid Single-Particle Lagrangian Integrated Trajectory) model. HYSPLIT is the newest version of a complete online system for computing simple air parcel trajectories to complex dispersion and deposition simulations for any location and date (depending on data availability) using a variety of standard data input products (e.g. the NCEP Reanalysis 1948-present).

Satellite smoke detection products were used to identify the spatial extent of smoke over the region (see <http://www.osdpd.noaa.gov/ml/land/fire.html>). These products show the detected hot spots and smoke plumes indicating possible fire locations and are based on algorithms for the C10904 GOES Imager, the POES, AVHRR and MODIS.

The AERONET (AERosol RObotic NETwork) is an inclusive federation of ground-based remote sensing networks. Measurements of vertically integrated aerosol properties are accomplished using a CIMEL sunphotometer/sky radiometer (Holben et al., 1998). The AERONET programmatic goals are to assess aerosol optical properties and validate satellite retrievals of aerosol optical properties (<http://aeronet.gsfc.nasa.gov/index.html>). AEROCAN CIMELs (AEROCAN is the Canadian sub-network of AERONET) have been important in tracing the transport and characteristics of Asian dust layers over British Columbia and, in general, over AEROCAN/AERONET sites across North America (e.g. Thulasiraman et al., 2001). The AEROCAN site on Saturna Island site (Fig. 1) is approximately 50 km south of Vancouver. The CIMEL instruments acquire solar irradiances which are transformed into three processing levels of Aerosol

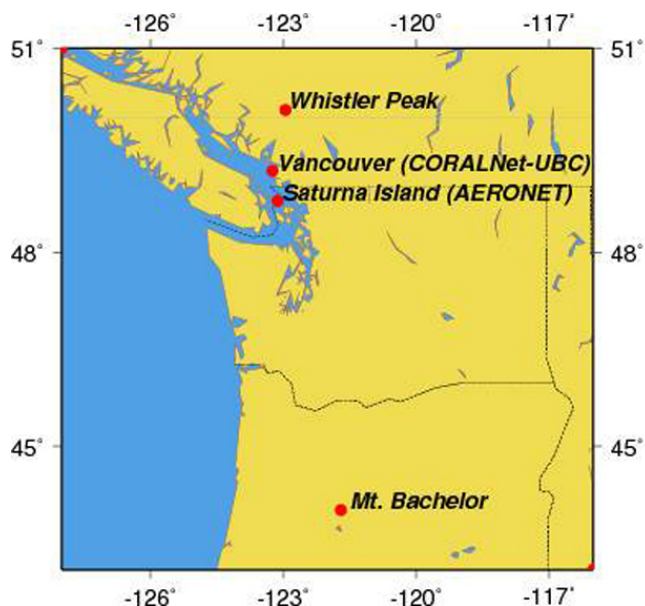


Fig. 1. Map of Western North America showing locations mentioned in the text.

Optical Thickness (AOT) (1.0 – non-cloud screened, 1.5 – cloud screened and 2.0 – cloud screened and quality assured) across eight spectral channels (340, 380, 440, 500, 670, 870, 1020 and 1640 nm). In a separate operational mode, almu-canter sky radiances are collected across four channels (440, 670, 870, and 1020 nm) at a nominal sampling resolution which is about 1/20 of the nominal AOT sampling resolution (an hour vs. 3 min). The sky radiances, along with AOT estimates at the same four channels, are used to perform inversions for particle size distribution and refractive index (Dubovik et al., 2000). In this paper we examine:

1. AOT at 500 nm (τ_{500}): this columnar parameter varies (extensively) with the vertically integrated aerosol number density and, in a second order fashion, (intensively) with average aerosol particle size in the column.
2. The partition of the τ_{500} into its fine and coarse mode optical depths at 500 nm. This is accomplished using spectral derivatives of the AOT spectrum (re the SDA algorithm of O'Neill et al., 2003). Fine mode (sub-micron) particles are generally associated with smoke and/or pollution aerosols while coarse mode (super-micron) particles generally indicate the presence of dust, marine aerosols and/or cloud particles.
3. Effective radius ($r_{\text{eff},f}$) of the fine mode size distribution (an intensive parameter). Dubovik's inversion code finds the minimum of the retrieved particle size distribution within the size interval from 0.194 to 0.576 μm . This minimum is used as a separation point between fine

and coarse mode particles. Fine and coarse mode optical thickness, phase function and asymmetry factor are then computed from the divided particle size distribution and the retrieved refractive index.

3 Results

3.1 Fire activity and meteorological factors

Wildfire activity in northern California during summer 2008 burned approximately 3,244.47 km² (worst on record) and included over 2,780 individual fires. A series of fires was triggered in northern California by lightning on 20 June and these continued throughout the summer. In early July and then again in early August, southerly winds carried dense smoke from the various fire complexes northward into Oregon, Washington State and British Columbia. Satellite based smoke detection products show extensive smoke haze spreading into southwestern British Columbia during the periods 30 June–3 July (Fig. 2a) and 4–7 August (Fig. 2b). Hysplit back-trajectories for both cases (red lines) indicate southerly flow and subsidence over the region.

Vertical soundings from Quillayute (western Olympic Peninsula, Washington State) for late afternoon 1 July and 6 August both show stable layers in the lower to mid-troposphere (the upper boundaries of which are indicated by red arrows in Fig. 3a, b). These layers are consistent with the top of the smoke haze layers detected by the CORALNet-UBC Lidar (Fig. 4) and likely acted as a vertical constraint to the smoke layer. Previous soundings (not shown here for brevity) indicate that the stable layer evident on 1 July had subsided from ~ 5000 m altitude over the previous 36 h. This is consistent with the decreasing altitude of the top of the smoke layer observed in CORALNet-UBC lidar imagery during 1 July (Fig. 4a).

3.2 Lidar and sunphotometer observations

CORALNet-UBC backscatter imagery provides a detailed representation of the time evolution of the vertical structure of the two smoke events (Fig. 4a, b, bottom panels) while the AOTs from the Saturna sunphotometer (Fig. 4a, b top panels, black symbols) can be visually interpreted as being proportional to the vertical integration of the backscatter coefficient (there are clearly transformations to be made in relating backscatter ratio at 1020 nm to aerosol extinction coefficient at 500 nm). The red and blue symbols of the top panels represent the fine and coarse mode contributions to the AOT. The Lidar backscatter at 1064 nm shows several features common to both events. In both cases, the regional smoke haze was evident to a height of ~ 5 km (the blue and green plumes in the backscatter imagery) although plume height varied somewhat through time. Furthermore, in each case, pronounced layering was evident within the lower troposphere (for example the layers depicted by green hues at 2 km around

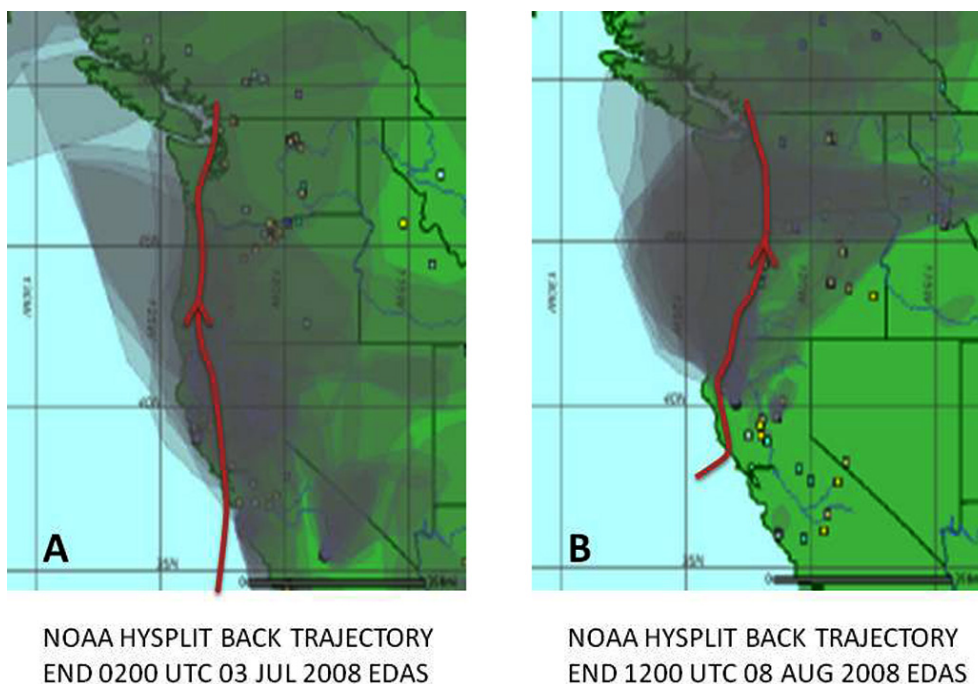


Fig. 2. Satellite smoke detections for (A) 30 June–3 July 2008 (B) 4–7 August 2008 with corresponding hysplit back trajectories shown by the red line. (Trajectory times correspond to the times of peak CO recorded at Whistler Peak and shown in Fig. 8).

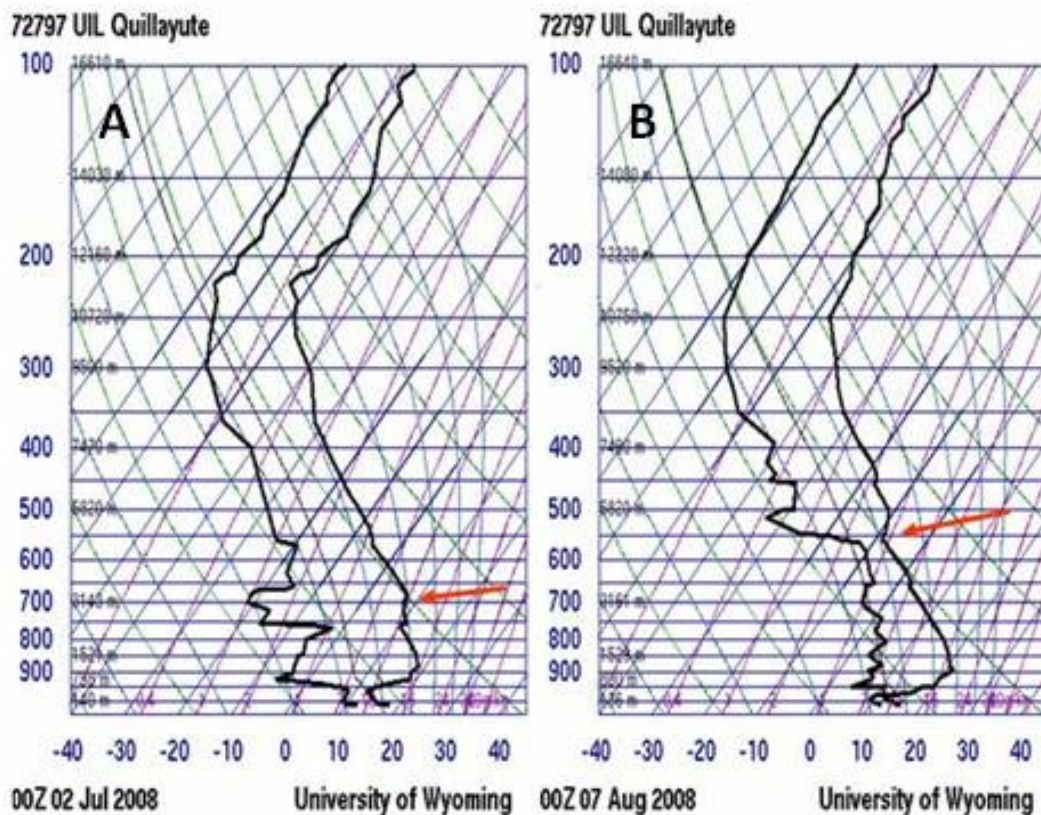


Fig. 3. Thermodynamic charts showing temperature and dew point profiles from Quillayute, Washington for late afternoon on 1 July (A) and 6 August (B) 2008. Red arrows shows height of inversion constraining the smoke plumes.

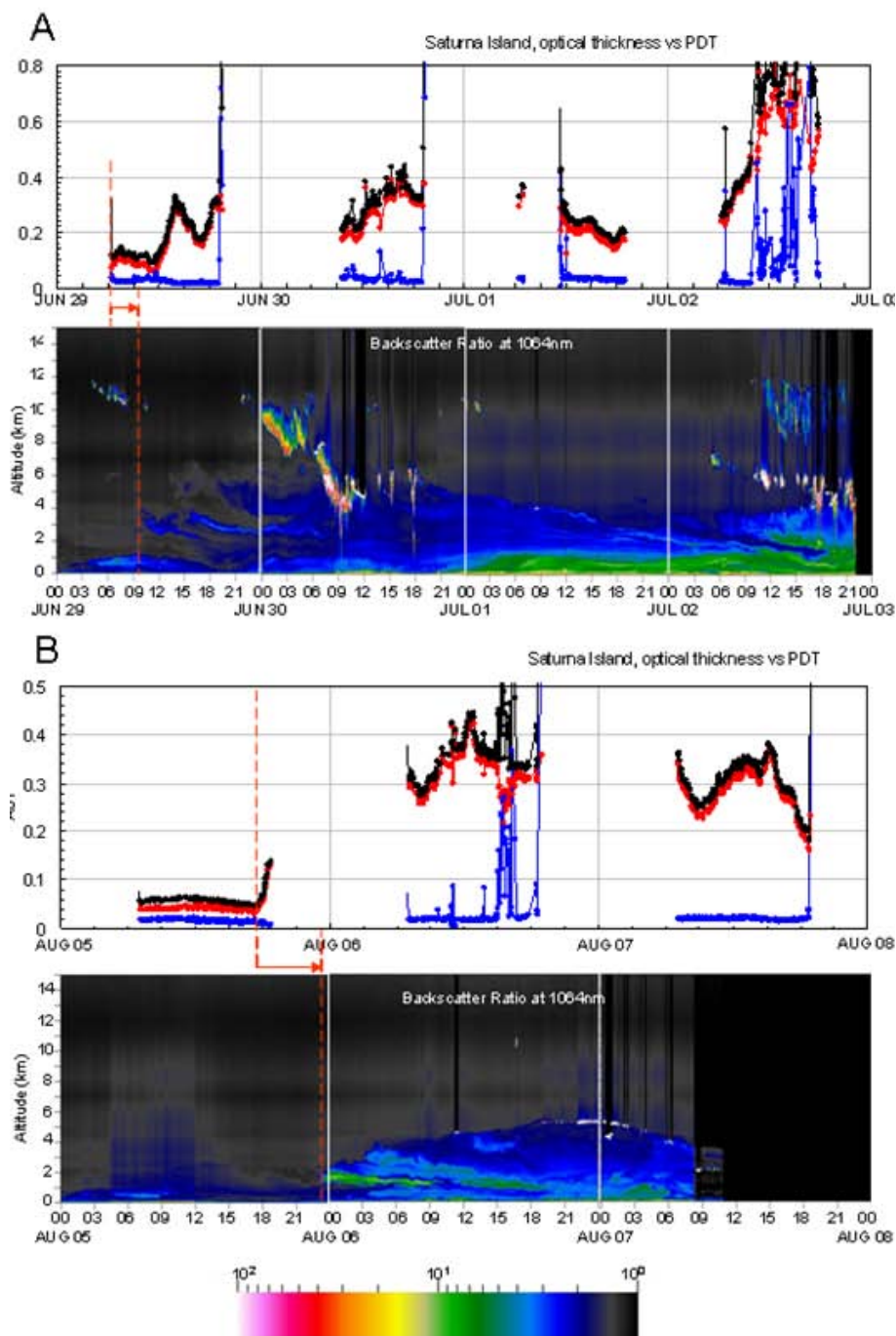


Fig. 4. Optical measurements for the smoke events of 29 June to 2 July and 5 August to 7 August. The top panels of (A) and (B) show day to day (500 nm) variation of AOT (black), fine mode optical depth (red) and coarse-mode optical depth (blue) while the bottom panels show temporally synchronized CORAL Net Lidar profiles of back scatter ratio (1064 nm). The SDA retrievals of fine and coarse mode optical depth were performed using the AERONET wavelength protocol of 380, 440, 500, 670, and 870 nm. Times are Pacific Daylight time (PDT = UT-7 h).

15:00 PDT on 2 July, and similarly, from 00:00 PDT on 6 August). Subsidence is also evident in both cases as indicated by decreasing height of specific layers through time. Finally, late in each event, the highest backscatter is shown near the

surface, suggesting that the plume has been mixed into the boundary layer. With respect to boundary layer entrainment, ground level concentrations of $\text{PM}_{2.5}$ at Vancouver International Airport reached $\sim 15 \mu\text{g m}^{-3}$ during both events (this

is \sim three times background concentrations). The highest $\text{PM}_{2.5}$ concentrations were recorded at Hope (eastern Lower Fraser Valley) on 2 July 2008 ($\sim 40 \mu\text{g m}^{-3}$). However, on 6–7 August $\text{PM}_{2.5}$ concentrations across the LFV did not exceed $15 \mu\text{g m}^{-3}$.

It is apparent in both cases shown in Fig. 4 that the AOT is dominated by fine-mode particles. This is supported by the depolarization ratio profiles which were universally low at the roughly sub-5km altitude range in which the smoke was located. Fine mode particles are typically characteristic of smoke; we conclude, given the cumulative evidence such as the lidar backscatter and depolarization profiles, backtrajectories, and satellite imagery that virtually all of the AOT variation, aside from the obvious high-frequency (thin-cloud) excursions of the coarse mode optical depth, is due to smoke.

In general the advection flow during the period of the two events was from the south or south west (roughly from the Saturna site to the CORALNet site). The presence of smoke (and cloud) would accordingly be registered at Saturna from ~ 1 to 6 h before the lidar depending on the altitude of a given plume filament and its actual detailed form across (what one typically has to presume) is a broad front \sim tens of kilometers in width. This time-lag, plume advection argument is usually non-trivial except in the simplest of cases. Figure 4 shows some examples of what we ascribed to Saturna AOTs leading the lidar backscatter profiles (red vertical lines and arrows). These are cases for which the advection was rudimentary (the smoke could be largely associated with a single narrow plume whose analysis was amenable to a simple forward trajectory analysis). Note that in the June 29 case, the elevated backscatter layer below ~ 1 km is contained within the urban boundary layer and largely comes from the Vancouver region (its influence on the optical depth would be much less at Saturna; the advection time lag indicated by the red lines is more likely associated with the plume which can be seen around 3 km altitude in the lidar profile).

Fine mode and total AOTs reached a maximum of ~ 0.7 on 2 July compared to a maximum ~ 0.4 on 6 August. These maxima are large but significantly less than reported cases of strong regional smoke events where the maximum AOTs at 500 nm were regularly $> \sim 1$ (see Eck et al. (2009) and O'Neill et al. (2005) for example). The Dubovik-retrieval values of $r_{\text{eff},f}$ during both the June/July and August events varied between about 0.13 and 0.15. Such values of $r_{\text{eff},f}$ are relatively small compared to values ~ 0.2 reported by O'Neill et al. (2005) (the curve labelled $r_{\text{eff},f,2}$ in Fig. 4a) for approximately two to three days of trajectory time (roughly the trajectory time of the California fires as per Fig. 2 above). Eck et al. (2009) show a strong dependence of the fine-mode volume median radius (a parameter whose value is typically slightly larger than $r_{\text{eff},f}$) with total optical depth (values varying between ~ 0.15 and ~ 0.25 for variations in AOT(440 nm) from ~ 0.2 to 3). The lower values or $r_{\text{eff},f}$ in the present study, compared to Eck et al. (2009) and O'Neill et al. (2005) are thus most likely attributable to

the lower optical depths characterizing this regional event. It is to be noted that we did examine single scattering albedo values generated by the Dubovik inversion given the optical (and radiative forcing) importance of this intensive parameter; however for the events we chose to investigate in this paper, no SSA values passed the Level 2.0 inversion criterion of $\text{AOD}(440 \text{ nm}) > 0.4$.

In Fig. 5, depolarization at 532 nm are shown for the two smoke events (Fig. 5b, c) and are contrasted with an example of trans-Pacific Asian dust transport observed at CORALNet-UBC on 25–26 April 2008 (Fig. 5a). Green-yellow-oranges hues in Fig. 5a depict subsiding multi-layer dust layers associated with Asian spring dust storms several days early and predicted to be transported across the region by the Naval Research Laboratory Aerosol global model (<http://www.nrlmry.navy.mil/aerosol/>). The characteristics and meteorology of such events are described in detail by McKendry et al. (2001, 2008). Aerosol depolarization for these layers is in the range 0.18–0.35 (18–35%) and are consistent with values measured elsewhere for Asian dust (e.g. Murayama et al., 2003; Sakai et al., 2003). In contrast, depolarization for both smoke events (Fig. 5b, c) shows little variability through the depth of the smoke haze layer and is in the range ~ 0.07 –0.14 (7–14%) (depicted by blue hues). These values are again consistent with values observed elsewhere and suggest that smoke particles were broadly spherical.

Corresponding CALIPSO depolarization imagery for the three cases is presented in Fig. 6a–c. Despite the obvious limitations induced by resolution as well as flight track (which does not put the instrument directly and consistently over CORALNet-UBC) both the dust event and the two smoke events of Fig. 5 are evident in the broad region (depicted by the red rectangles), and have aerosol layer elevations and depolarization ratios that are consistent with CORALNet-UBC. In Fig. 7a–c, CALIPSO aerosol sub-type products confirm the presence of dust over the region for the April event and smoke for the July and August aerosol events.

3.3 Mountaintop chemistry

Chemistry observations from both Mt Bachelor and Whistler (Fig. 8) provide an important complement to remote sensing data examined in previous sections. At Mt Bachelor (Fig. 8a), aerosol scattering data suggests that the early July smoke event persisted over several days with peak CO and O₃ values of 470 and 80 ppbV respectively. In contrast, the early August event (Fig. 8b) was of shorter duration (based on aerosol scattering) but of higher magnitude with peak CO concentrations reaching 550 ppbV on 8 August 2008. CO and O₃ measurements at Whistler (Fig. 8c, d) are of comparable magnitude to those observed at Mt. Bachelor for both events.

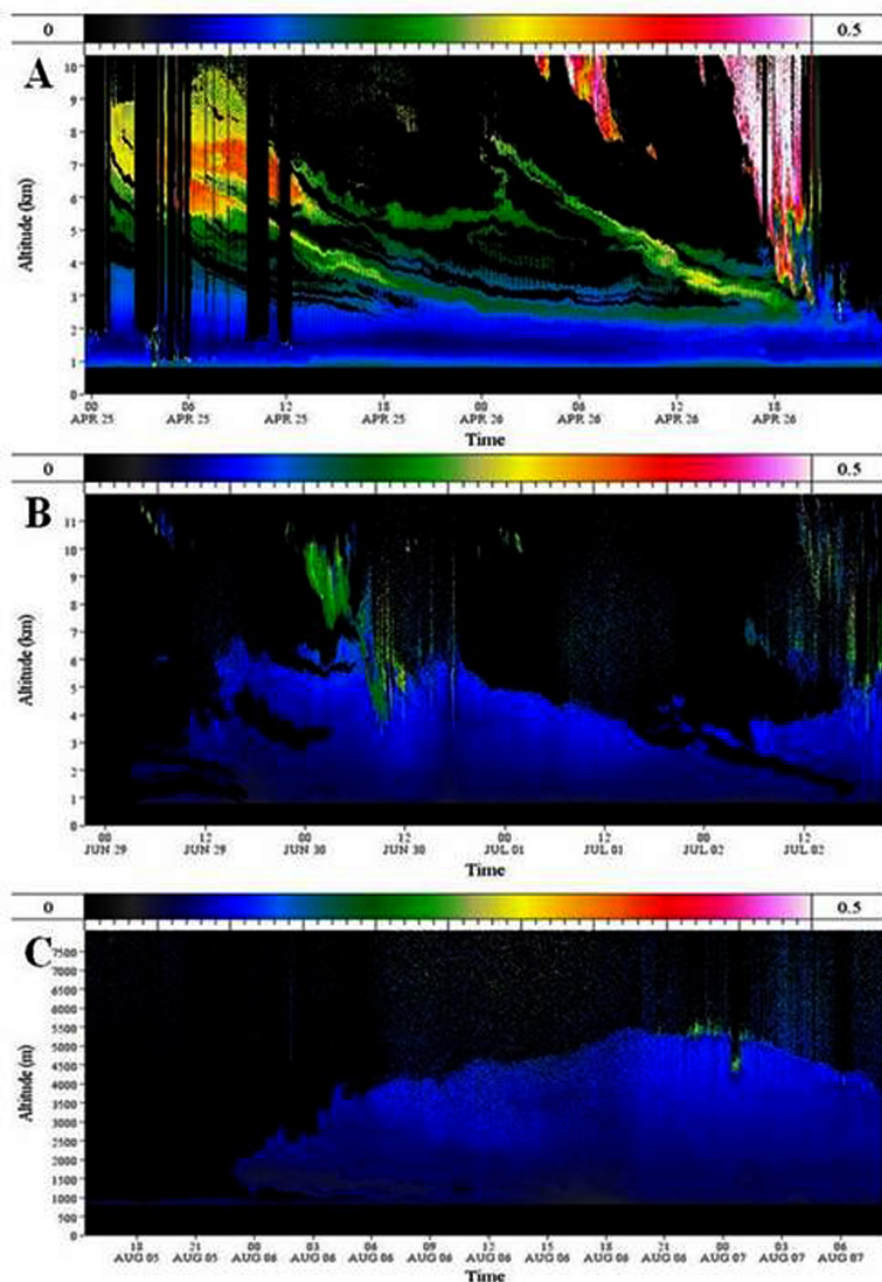


Fig. 5. CORALNet-UBC lidar Depolarization ratios for (A) Asian dust event on 26 April 2008 (note dust layers shown by green/yellow/orange hues subsiding with time) (B) Smoke plume (blue hues) on 29 June–2 July 2008 and (C) smoke plume on 5 August–7 August 2008.

A comparison of optical and particle number concentrations from the April dust event and the August smoke event are shown in Fig. 9; particle scattering and number concentrations are not available at Whistler for the July 2008 smoke event. In Fig. 9 are shown particle absorption coefficient, green light scattering coefficient, ratio of green backscatter coefficient to the green light scattering coefficient, particle

number concentration $> 1 \mu\text{m}$ and particle number concentration $> 500 \text{ nm}$. The contribution of particles $> 0.5 \mu\text{m}$ relative to those $> 1 \mu\text{m}$ was somewhat higher during the August fire event than during the April dust event, consistent with the Saturna Island sunphotometer observations as well as other studies reviewed by Reid et al. (2005a, b) that show smoke particles reside overwhelmingly in the accumulation mode.

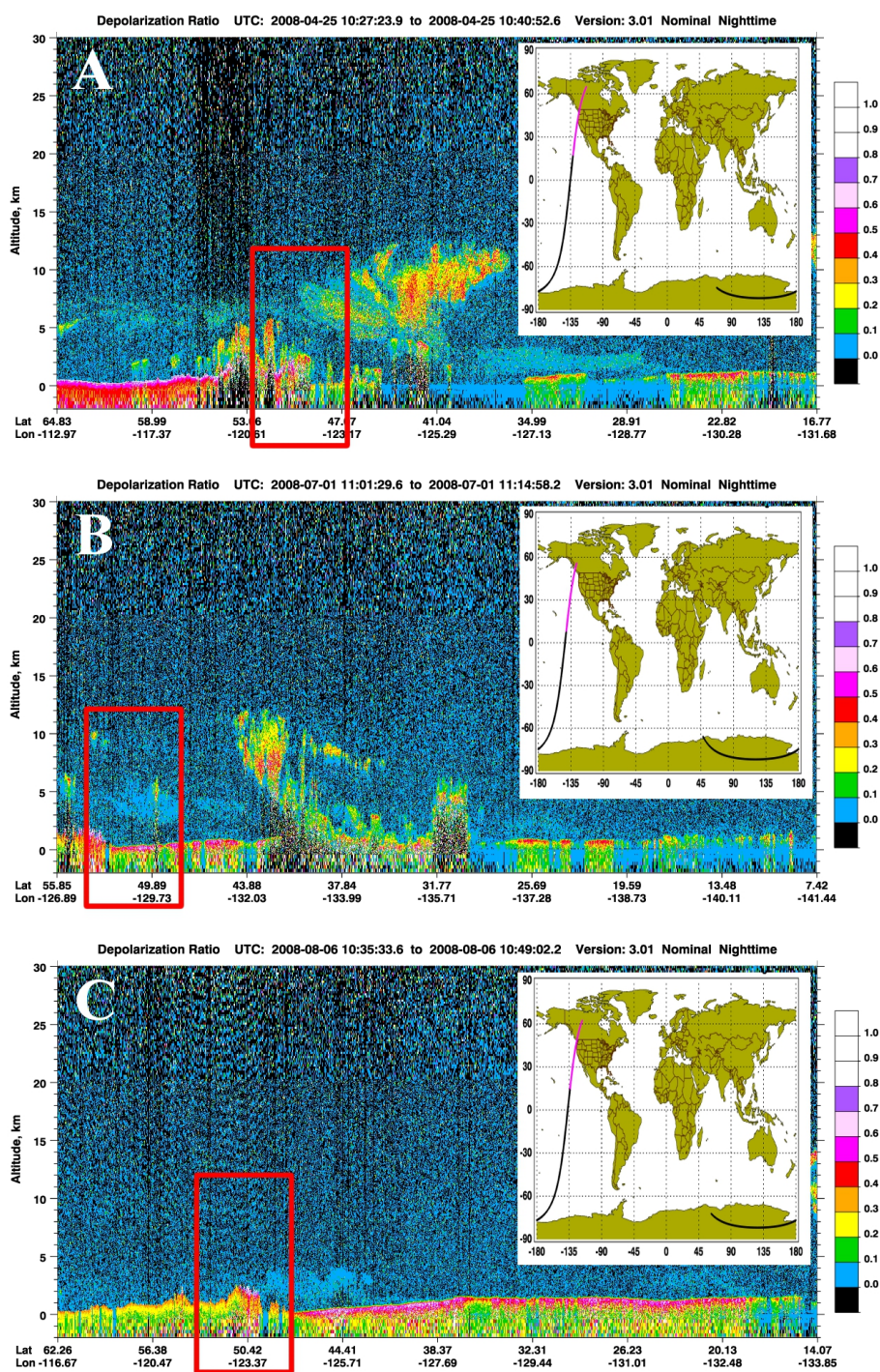


Fig. 6. CALIPSO lidar depolarization ratios corresponding to the three cases shown in Fig. 5: (A) 26 April 2008 Dust event (note green and yellow hues in Red square) (B) 1 July 2008 smoke event (note blue hues in red square) and (C) 6 August 2008 smoke event (note blue hues in red square). Red squares represent approximate location of CORALNet-UBC. Satellite paths are shown on maps to right. Minimum distances of the satellite paths from CoralNet-UBC were 25 April 2008 70 km ESE; 1 July 2008, 470 km NW; 4 August 2008, 4 km WNW.

During both the dust event and the smoke event, the increases in the particle absorption and scattering at Whistler correspond closely with the increases in the particle number concentrations. The measured particle scattering and ab-

sorption coefficients are 4–5 times higher during the smoke event than the April dust event. The relative difference in the particle number concentrations is much less, suggesting that the scattering and absorption efficiencies of the aerosol

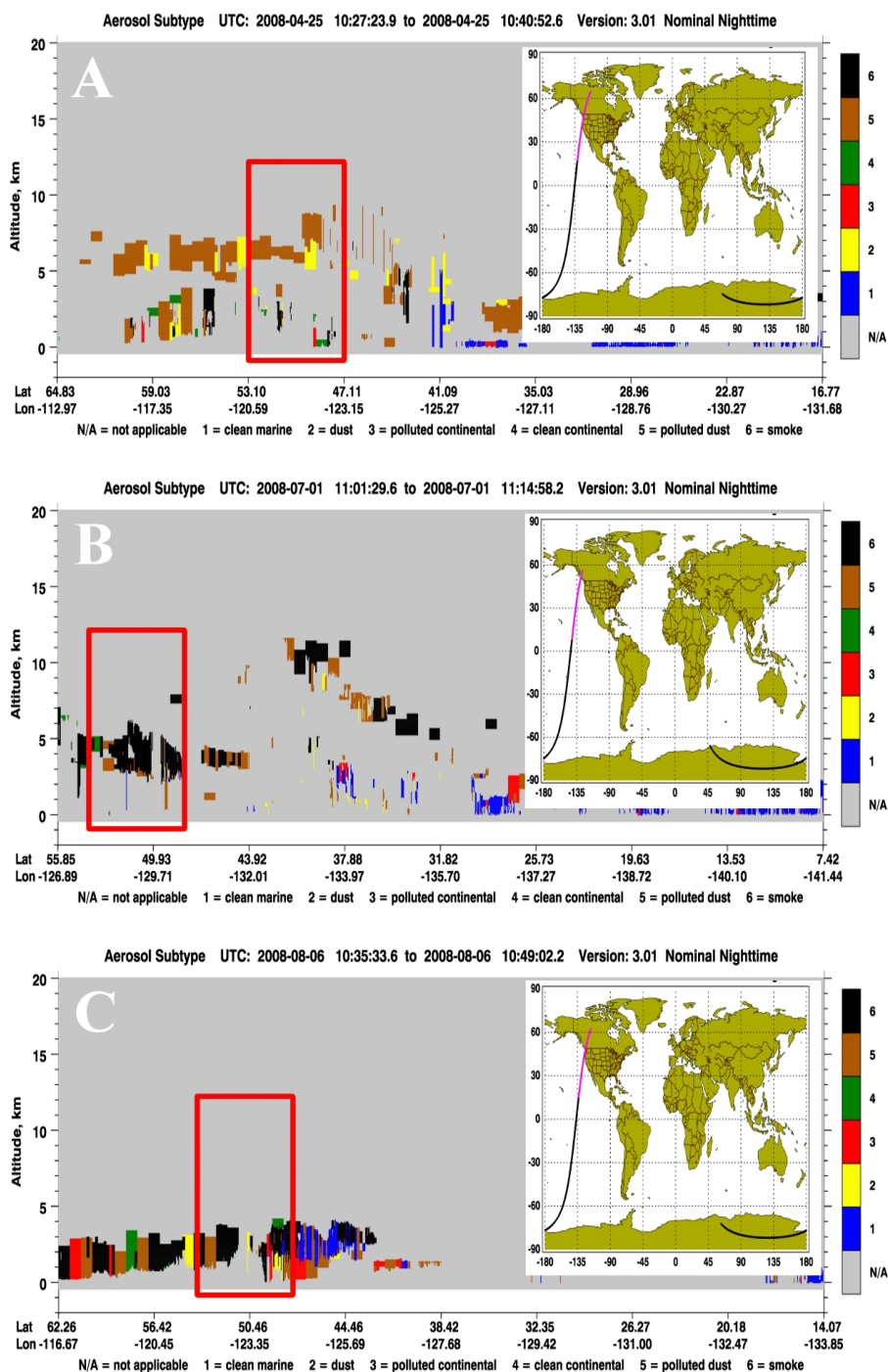


Fig. 7. CALIPSO aerosol subtypes corresponding to the three cases shown in Figs. 5 and 6 (A) 26 April 2008 Dust event (B) 1 July 2008 smoke event and (C) 6 August 2008 smoke event. Red squares represent approximate location of CORALNet-UBC. Satellite paths are shown on maps to right.

during the dust-event aerosol were greater than the fire-event aerosol; unfortunately, the DMA component of the WSP ($<0.5\ \mu\text{m}$) was not operational during these periods. The ratio of the scattering to absorption coefficients is about 15–20 for the August fire event compared with a value of about

10 for the April dust event. The single scatter albedos estimated from these measurements are 0.91 and 0.94 for the dust event and smoke event, respectively. The nephelometer does not accurately measure the light scattering by particles $>$ about $1\ \mu\text{m}$ due to the enhanced forward scattered

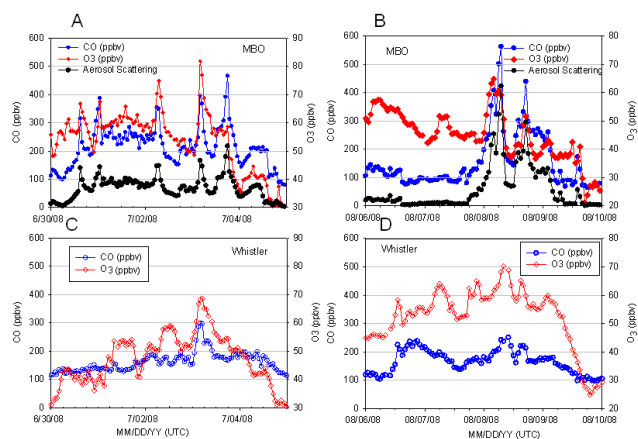


Fig. 8. Mountain-top CO and O₃ observations at Mount Bachelor (MBO) (A and B) and Whistler Mountain (C and D) for 1 July smoke event (left panels) and 6 August smoke events (right panels). Aerosol scattering is also shown for MBO.

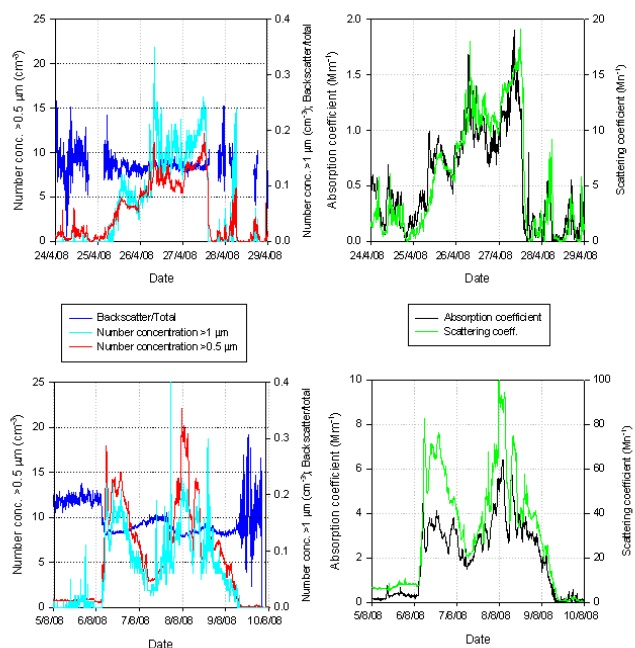


Fig. 9. Optical and particle number concentrations from the April dust event (top panels) and the August smoke event (bottom panels) at Whistler Mountain; data were not available for the July 2008 smoke event.

light by such particles that is not sufficiently collected by the nephelometer optical configuration (e.g. Anderson and Ogren, 1998), and thus contributions from the larger particles are underestimated.

For the dust event, the ratio of the backscattered light to the total scatter is slightly lower than during the smoke event. This is consistent with enhanced forward scatter by the relatively higher contribution from larger particles. During the

August smoke event, the ratio of the backscattered light to the total scatter decreased compared with the value of the ratio for the much lower aerosol concentrations before, indicative of a greater influence of larger particles on the scattering during these specific events relative to the cleaner free-troposphere aerosol. Finally, filter pack measurements at Whistler Mountain were available for the two smoke events only and show elevated K/to SO₄ ratios (0.05 and 0.06 respectively). This is consistent with other observations of smoke (Reid et al., 2005b) where enhanced K is noted as a marker of biomass burning.

4 Discussion and conclusions

A severe forest fire season in 2008 in Northern California and Oregon was responsible for two significant regional scale transport events observed in southern British Columbia. A combination of ground based (CORALNet) and satellite (CALIPSO) lidar, sunphotometry and high altitude chemistry observations permitted unprecedented characterization of forest fire plume height and mixing as well as optical and physico-chemical characteristics.

The transported smoke when observed in southwestern BC for the 1 July and 6 August events was observed by lidar to be mixed through a layer extending to 5–6 km a.g.l. where the smoke was confined by an elevated inversion. Coherent layered structures were apparent in the plume. Depolarization ratios for a dust event and the two smoke events were consistent with observations of dust and smoke events elsewhere and provide basis for discrimination of aerosol events in the region.

Based on sunphotometry, fine mode and total AOTs reached a maximum of ~ 0.7 on 2 July compared to a maximum ~ 0.4 on 6 August. These maxima are large but significantly less than reported cases of strong regional smoke events where the maximum AOTs at 500 nm were regularly $> \sim 1$. Dubovik-retrieval values of $r_{\text{eff},f}$ during both the June/July and August events varied between about 0.13 and 0.15 μm and confirm the dominance of accumulation mode size particles in the forest fire plumes. Both Whistler Peak and MBO data show that smoke events are accompanied by elevated CO and O₃ concentrations as well as elevated K⁺/SO₄ ratios. With respect to physico-chemical characteristics, the two cases of medium-range smoke transport described herein are therefore broadly consistent with observations elsewhere and summarized by Reid et al. (2005a, b).

In addition to documenting the meteorology and physico-chemical characteristics of two regional scale biomass burning plumes, this study demonstrates the positive analytical synergies arising from the suite of measurements now in place in the Pacific Northwest, and complemented by satellite borne instruments. It is expected that these facilities in combination will contribute significantly to scientific understanding of the meteorological processes and transformations

associated with regional aerosol transport. In addition to the policy implications of such sound scientific knowledge, it is anticipated that this research will provide a basis for the provision of timely public information and warnings related to aerosol pollution. This capacity will likely assume greater significance due to projected increases in forest fire frequency and severity in western North America under Climate Change scenarios.

Acknowledgements. We are grateful for the financial and in-kind support provided by Environment Canada, the Natural Sciences and Engineering Research Council, the BC Ministry of Environment, and the Canadian Foundation for Climate and Atmospheric Sciences. Special thanks also go to the University of British Columbia and in particular to Seane Trehearne at Totem Field, and Michael Travis and Bernard Firanski of Environment Canada. We are grateful for the constructive suggestions of two anonymous referees.

Edited by: N. Mihalopoulos

References

- Amiridis, V., Balis, D. S., Giannakaki, E., Stohl, A., Kazadzis, S., Koukoulis, M. E., and Zanis, P.: Optical characteristics of biomass burning aerosols over Southeastern Europe determined from UV-Raman lidar measurements, *Atmos. Chem. Phys.*, 9, 2431–2440, doi:10.5194/acp-9-2431-2009, 2009.
- Anderson, T. L. and Ogren, J. A.: Determining aerosol radiative properties using the TSI 3563 integrating nephelometer, *Aerosol Sci. Tech.*, 29, 57–69, 1998.
- Bond, T. C., Anderson, T. L. and Campbell, D.: Calibration and Intercomparison of Filter-Based Measurements of Visible Light Absorption by Aerosols, *Aerosol Sci. Technol.*, 30, 582–600, 1999.
- Dubovik, O. and King, M. D.: A flexible inversion algorithm for retrieval of aerosol optical properties from Sun and sky radiance measurements, *J. Geophys. Res.*, 105, 20673–20696, 2000.
- Duck, T. J., Firanski, B. J., Millet, D. B., Goldstein, A. H., Allan, J., Holzinger, R., Worsnop, D. R., White, A. B., Stohl, A., Dickinson, C. S., and van Donkelaar, A.: Transport of forest fire emissions from Alaska and the Yukon Territory to Nova Scotia during summer 2004, *J. Geophys. Res.-Atmos.*, 112, D10S44, doi:10.1029/2006JD007716, 2007.
- Eck, T. F., Holben, B. N., Hyer, E. J., Reid, J. S., Shaw, G. E., Sinyuk, A., Vande Castle, J. R., Chapin, F. S., O'Neill, N. T., Dubovik, O., Smirnov, A., Vermote, E., Schafer, J. S., Giles, Slutsker, I., Sorokine, M., and Newcomb, W.: Optical Properties of Boreal Region Biomass Burning Aerosols In Alaska and Transport of Smoke to Arctic Regions, *J. Geophys. Res.*, 114, D11201, doi:10.1029/2008JD010870, 2009.
- Hacker, J. P., McKendry, I. G., and Stull, R. B.: Modeled downward transport of Asian dust over Western North America during April 1998, *J. Appl. Met.*, 40, 1617–1628, 2001.
- Hoff, R. M., Torres, O., Delgado R., and Rogers, R.: Lidar validation of Calipso and OMI using ground-based sensors from Realm. Third Symposium on LIDAR atmospheric Applications, The 87th AMS Annual Meeting (San Antonio, TX) 13–18 January, 2007.
- Holzer, M., McKendry, I. G., and Jaffe, D. A.: Spring-time Trans-Pacific atmospheric transport from East Asia: A transit-time-PDF approach, *J. Geophys. Res.*, 108(D22), 4708, doi:10.1029/2003JD003558, 2003.
- Jaffe, D., McKendry, I., Anderson, T., and Price, H.: Six 'New' Episodes of Trans-Pacific Transport of Air Pollutants, *Atmos. Environ.*, 37(3), 391–404, 2003.
- Leaith, W. R., Macdonald, A. M., Anlauf, K. G., Liu, P. S. K., Toom-Saunty, D., Li, S.-M., Liggio, J., Hayden, K., Wasey, M. A., Russell, L. M., Takahama, S., Liu, S., van Donkelaar, A., Duck, T., Martin, R. V., Zhang, Q., Sun, Y., McKendry, I., Shantz, N. C., and Cubison, M.: Evidence for Asian dust effects from aerosol plume measurements during INTEX-B 2006 near Whistler, BC, *Atmos. Chem. Phys.*, 9, 3523–3546, doi:10.5194/acp-9-3523-2009, 2009.
- Kahn, R. A., Chen, Y., Nelson, D. L., Leung, F.-Y., Li, Q., Diner, D. J., and Logan, J. A.: Wildfire smoke injection heights: Two perspectives from space, *Geophys. Res. Lett.*, 35, L04809, doi:10.1029/2007GL032165, 2008.
- Kittaka, C., Pierce, B., Schaack, T., Al-Saadi, J., Soja, A., Tripoli, G., da Silva, A., Szykman, J., Lambeth, B. and Winker, D.: Synthesis of multiple observations using a regional aerosol assimilation/forecast model (RAQMS) and assessment of biomass burning emission estimates, 16th Annual International Emission Inventory Conference Emission Inventories: "Integration, Analysis, and Communications", available at: <http://www.epa.gov/ttn/chief/conference/ei16/index.html#ses-10>, Raleigh, May 14–17, 2007.
- McKendry, I. G., Hacker, J. P., Stull, R., Sakiyama, S., Mignacca, D., and Reid, K.: Long range transport of Asian dust to the Lower Fraser Valley, British Columbia, Canada, *J. Geophys. Res.*, 106(D16), 18361–18370, 2001.
- McKendry, I. G., Strawbridge, K. O'Neill, N., Macdonald, A. M., Liu, P., Leaith, W. R., Anlauf, K., Jaegle, L., Jaffe, D., Fairlie, D., and Westphal, D.: A Case of Trans-Pacific Transport of Saharan Dust to Western North America, *J. Geophys. Res.* 112, D01103, doi:10.1029/2006JD007129, 2007.
- McKendry, I. G., Macdonald, A. M., Leaith, W. R., van Donkelaar, A., Zhang, Q., Duck, T., and Martin, R. V.: Trans-Pacific dust events observed at Whistler, British Columbia during INTEX-B, *Atmos. Chem. Phys.*, 8, 6297–6307, doi:10.5194/acp-8-6297-2008, 2008.
- Murayama, T., Müller, D., Wada, K., Shimizu, A., Sekiguchi M., and Tsukamoto, T.: Characterisation of Asian dust and Siberian smoke with multi-wavelength Raman lidar over Tokyo, Japan in spring 2003, *Geophys. Res. Lett.*, 31, L23103, doi:10.1029/2004GL021105, 2004.
- O'Neill, N. T., Eck, T. F., Smirnov, A., Holben, B. N., and Thulasiraman, S.: Spectral discrimination of coarse and fine mode optical depth, *J. Geophys. Res.*, 108(D17), 4559–4573, doi:10.1029/2002JD002975, 2003.
- O'Neill, N. T., Thulasiraman, S., Eck, T. F., and Reid, J. S.: Robust optical features of fine mode size distributions; application to the Québec smoke event of 2002, *J. Geophys. Res.*, 110(D11), D11207, doi:10.1029/2004JD005414, 2005.
- O'Neill, N. T., Pancrati, O., Baibakov, K., Eloranta, E., Batchelor, R. L., Freemantle, J., McArthur, L. J. B., Strong, K., and Lindenmaier, R.: Occurrence of weak, sub-micron, tropospheric aerosol events at high Arctic latitudes, *Geophys. Res. Lett.*, 35, L14814,

- doi:10.1029/2008GL033733, 2008.
- Pahlow, M., Kleissl, J., Parlange, M. B., Ondov, J. O., and Harrison, D.: Atmospheric boundary-layer structure observed during a haze event due to forest-fire smoke, *Bound.-Lay. Meteorol.*, 114, 53–70, 2005.
- Reid, J. S., Eck, T. F., Christopher, S. A., Koppmann, R., Dubovik, O., Eleuterio, D. P., Holben, B. N., Reid, E. A., and Zhang, J.: A review of biomass burning emissions part III: intensive optical properties of biomass burning particles, *Atmos. Chem. Phys.*, 5, 827–849, doi:10.5194/acp-5-827-2005, 2005a.
- Reid, J. S., Koppmann, R., Eck, T. F., and Eleuterio, D. P.: A review of biomass burning emissions part II: intensive physical properties of biomass burning particles, *Atmos. Chem. Phys.*, 5, 799–825, doi:10.5194/acp-5-799-2005, 2005b.
- Sakai, T., Nagai, T., Nakazato, M., Mano, Y., and Matsumura, T.: Ice Clouds and Asian Dust Studied with Lidar Measurements of Particle Extinction-to-Backscatter Ratio, Particle Depolarization, and Water-Vapor Mixing Ratio over Tsukuba, *Appl. Optics*, 42, 7103–7116, 2003.
- Sassen, K.: Lidar Backscatter Depolarization Technique for Cloud and Aerosol Research, in: “Light Scattering by Nonspherical Particles: Theory, Measurements, and Geophysical Applications”, edited by: Mishchenko, M. L., Hovenier, J. W., and Travis, L. D., Academic Press, ISBN0-12-498660-9, 393–416, 2000.
- Thulasiraman, S., O’Neill, N. T., Royer, A., Holben, B. N., Westphal, D. L., and McArthur, L. J. B.: Sunphotometric observations of the 2001 Asian dust storm over Canada and the US, *Geophys. Res. Lett.*, 29(8), 1255–1258, doi:10.1029/2001GL014188, 2002.
- Vaughan, M. A., Powell, K. A., Winker, D. M., Hostetler, C. A., Kuehn, R. E., Hunt, W. H., Getzewich, B. J., Young, S. A., Liu, Z., and McGill, M. J.: Fully Automated Detection of Cloud and Aerosol Layers in the CALIPSO Lidar Measurements, *J. Atmos. Ocean. Technol.*, 26(10), 2034–2050, 2009.
- Weiss-Penzias, P., Jaffe, D., Swartzendruber, P., Hafner, W., Chand, D., and Prestbo, E.: Quantifying atmospheric mercury emissions from biomass burning and East Asian industrial regions based on ratios with carbon monoxide in pollution plumes at the Mount Bachelor Observatory, *Atmos. Environ.*, 41, 4366–4379, doi:10.1016/j.atmosenv.2007.1001.1058, 2007.